Photogeneration Action Spectroscopy of Neutral and Charged Excitations in Films of a Ladder-Type Poly(Para-Phenylene)

M. Wohlgenannt,[1,3] W. Graupner,[2,3] G. Leising,[3] and Z. V. Vardeny[1]

[1]*Department of Physics, University of Utah, Salt Lake City, Utah 84112*
[2]*Department of Physics, Virginia Tech, Blacksburg, Virginia 24061-0435*
[3]*Institut für Festkörperphysik, Technische Universität Graz, Petersgasse 16, A-8010 Graz, Austria*

The photogeneration quantum efficiency action spectra of long-lived neutral and charged excitations in films of a ladder-type poly(para-phenylene) were measured. We found that both triplet and polaron action spectra show, in addition to a step function increase at the optical gap, a monotonic rise at higher energies. For triplets this rise is explained by singlet exciton fission into triplet pairs from which the triplet exciton energy in the gap was obtained; this energy was also confirmed by measuring the weak phosphorescence band. For polarons the photogeneration increase at high energies is modeled by a novel hot electron interchain tunneling process.   [S0031-9007(99)08980-2]

The photogeneration dynamics of singlet excitons and secondary photoexcitations, such as triplets and polarons, in π-conjugated polymers have been usually measured by picosecond transient spectroscopic techniques rather than cw spectroscopies, since their photogeneration processes usually occur in the subnanosecond time domain [1]. On the other hand, the excited states energy levels of these polymers are often measured by cw optical techniques including electroabsorption [2], resonant Raman scattering [3], and by two and three photon nonlinear optical spectroscopies [4]. In this Letter we employ a new version of the cw photomodulation (PM) spectroscopy technique, which is capable of measuring the photogeneration quantum efficiency, η, of long-lived secondary photoexcitations without the need of transient optical techniques. We show that when the PM signal is measured under conditions far from the steady state, then it directly correlates with η; therefore the PM action spectrum (PMAS) measured under these conditions gives the dependence of η on the excitation photon energy, E, i.e., $\eta(E)$.

We have used the PMAS technique to obtain $\eta(E)$ of singlet and triplet excitons and polarons, respectively, in films of methyl-substituted ladder-type poly(para-phenylene) (mLPPP) [5] shown in Fig. 1, inset. mLPPP is an attractive π-conjugated polymer for blue-light emitting devices [6] due to its high photoluminescence (PL) quantum yield; this is caused, in part, by the intrachain order in the film induced by the planarization of neighboring phenyl rings [7]. mLPPP was chosen as a model polymer because of its reduced inhomogeneity and small defect density [8].

For the excitation beam in the PMAS measurements we used either an Ar^+ laser at several discrete E, or a monochromatized xenon lamp beam to continuously vary E between 2 and 4.5 eV. The excitation beam was modulated with a chopper at a frequency, f, between 10 to 4 kHz. A combination of various incandescent lamps, diffraction gratings, optical filters, and solid state detectors was used to span the probe energy ($\hbar\omega$) between 0.1 and 3 eV. The PM spectrum as a function of $\hbar\omega$ was obtained by dividing the pump beam induced changes in transmission, $\Delta T(\omega)$, by the probe transmission $T(\omega)$, where $\Delta\alpha = -d^{-1}\Delta T/T$ and d is the film thickness; ΔT was measured by a phase sensitive technique at f.

We first show how to directly obtain $\eta(E)$ for various excitations in the PM spectrum from the cw PMAS measurements. $\Delta\alpha$ is proportional to the photoexcitation density, N, via the relation $\Delta\alpha = N\sigma$, where σ is the
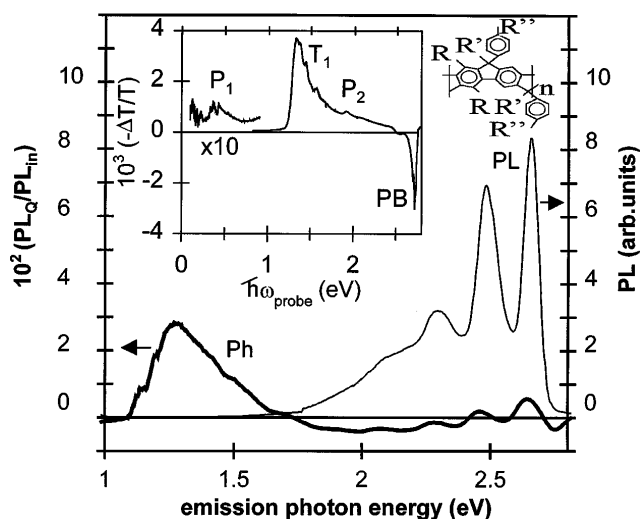

FIG. 1. The emission spectra of a mLPPP film measured in-phase $(PL)_{in}$ (thin line) and in quadrature $(PL)_Q$ (bold line) at 80 K, excited at 3.5 eV, and modulated at 3.5 kHz. $(PL)_{in}$ spectrum shows the uncorrected PL band, whereas $(PL)_Q/(PL)_{in}$ shows the phosphorescence (Ph) band. The left inset is the in-phase photomodulation spectrum at 80 K, excited at 3.5 eV, and modulated at 100 Hz. The triplet (T_1), polaron (P_1 and P_2), photobleaching (PB) bands are assigned. The right inset shows the repeat unit of the mLPPP polymer.

excitation optical cross section. Since $\Delta\alpha \sim \Delta T$, it follows that the changes in the probe transmission measured in phase, ΔT_{in}, and quadrature, ΔT_Q, to the laser beam modulation at f may be directly related to N dynamics, where $\Delta T_{in} \sim N_{in}$ and $\Delta T_Q \sim N_Q$. The two N components, N_{in} and N_Q may be calculated, in principle, from the modulated excitation intensity, $I(t)$, which is a periodic square wave in time with an illuminating pulse duration $t_0 = 1/2f$, using the rate equation

$$\frac{dN}{dt} = \eta g I - \beta N \qquad (1)$$

for a monomolecular recombination (MR) process. For bimolecular recombination (BR) the βN term in Eq. (1) is replaced by γN^2. Here β and γ are the MR and BR constants, respectively. We obtained [9] analytic expressions for the two N components in the limiting cases of steady state and far from the steady state, where steady state is defined by the condition $f\tau \ll 1$, and far from it by $f\tau \gg 1$; here τ is the decay time of the long-lived photoexcitations, i.e., $\tau = 1/\beta$ and $\tau = 1/\gamma N$ for MR and BR kinetics, respectively. From our calculations we found, in particular, that far from the steady state ($f\tau \gg 1$) $N_Q = I g \eta/2f$, and thus N_Q *is independent of* τ. Since τ depends on the recombination kinetics and on various external parameters such as temperature and excitation density, then the *absence of* τ *in the above expression for* N_Q *is essential for the direct determination of* η from cw measurements. To obtain $\eta(E)$ we first measure the PMAS as a function of E, namely, the excitation spectrum of a PM band (at a fixed $\hbar\omega$) normalized by the absorbed photons. For this we multiplied the pump intensity $I(E)$ by the factor $g(E) = 1/(Ed)(1 - R)[1 - \exp(-\alpha d)]$, where $R(E)$ and $\alpha(E)$ are the film reflectivity and absorption coefficient, respectively. Then the PMAS measured under conditions far from the steady state, namely, $\Delta T_Q(E)/gI$ at $f\tau \gg 1$, is directly proportional to $\eta(E)$.

We now identify the various photoexcitations in the mLPPP PM spectrum. The inset of Fig. 1 shows the PM spectrum as a function of the probe $\hbar\omega$ of a spin-cast mLPPP film at 80 K excited at 3.5 eV, measured in-phase at 100 Hz. The PM spectrum is dominated by the photoinduced absorption (PA) band T_1 at 1.3 eV and also by the two correlated PA bands: P_1 and P_2 at 0.4 and 1.9 eV, respectively. A series of photoinduced infrared-active vibrations (IRAV) that are correlated by their f and temperature dependencies with the PA bands P_1 and P_2, but not with T_1, are also seen at $\hbar\omega < 0.25$ eV [10]. The photobleaching feature in Fig. 1 marks the mLPPP optical gap, $E_{op} \simeq 2.6$ eV [11]. The photoinduced IRAVs indicate that charge carriers are photogenerated on the polymer chains. Their correlation with P_1 and P_2, but not with T_1 shows, therefore, that the former bands are due to long-lived *charged* excitations, whereas the latter band is caused by long-lived *neutral* excitations. In fact, the P_1 and P_2 bands coincide in energy with the two dop-

ing induced absorption bands in mLPPP films caused by polarons [10]. Also from studies of long-lived photoexcitations of isolated PPP oligomers, T_1 can be assigned to a triplet-triplet ($T - T^*$) transition [7]. We therefore conclude that P_1 and P_2 PA bands are due to photogenerated polarons, whereas T_1 is caused by photoexcited triplet excitons.

Using the PMAS technique as discussed above we obtained $\eta(E)$ for the PL band and T_1 and P_1 PA bands, respectively. To obtain $\eta_{PL}(E)$ we determined the absolute value of the PL quantum efficiency using an integrating sphere; we found $\eta_{PL} \simeq 30\%$ at $E = 3.5$ eV. From this value and the PL excitation spectrum, detected at $\hbar\omega = 2.2$ eV (Fig. 1), we obtained $\eta_{PL}(E)$ as shown in Fig. 2, inset. It is seen that $\eta_{PL}(E)$ abruptly increases at $E = 2.4$ eV, followed by a constant value at higher E. This step function behavior is similar to $\eta_{PL}(E)$ measured in the best poly(phenylene-vinylene) films [12], and shows that singlet excitons are the primary excitations in mLPPP, as can also be inferred from the large exciton binding energy ($\simeq 0.5$ eV) obtained for this polymer [11]. The $\eta_{PL}(E)$ spectrum may be explained as follows: Hot excitons thermalize down to the lowest lying singlet exciton level on a time scale of the order of 1 ps, whereas the PL emission from this exciton typically occurs in time of order 100 ps following the excitation [13]. Since singlet excitons recombine radiatively with a given quantum efficiency, then the η_{PL} spectrum reflects the η spectrum for singlet excitons, which is close to 1 in mLPPP, independent of E.

The triplet photogeneration quantum efficiency, $\eta_T(E)$, obtained by measuring $\Delta T_Q(E)/gI$ for the T_1 band at
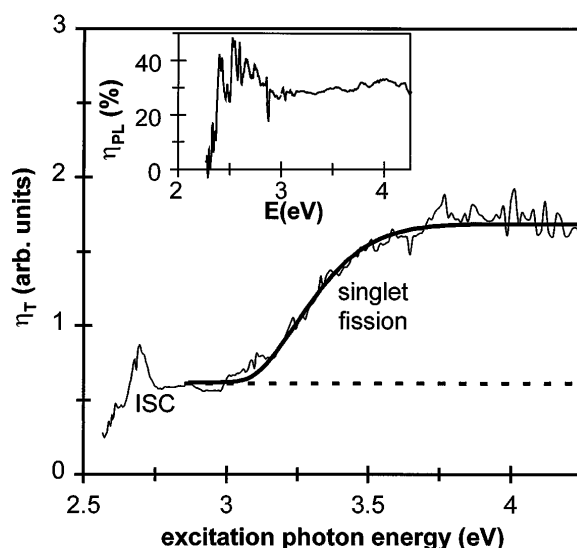

FIG. 2. The triplet action spectrum, $\eta_T(E)$. The bold line through the data points is a theoretical fit using a model of singlet fission. ISC is the process of triplet photogeneration via intersystem crossing. The dotted line illustrates $\eta_T(E)$ separation into the two photogeneration processes. The inset shows the PL action spectrum, $\eta_{PL}(E)$.

$\hbar\omega = 1.3$ eV (Fig. 1, inset), is shown in Fig. 2. $\eta_T(E)$ also has a step function response at $E = E_{\text{op}}$ similar to $\eta_{\text{PL}}(E)$; however, $\eta_T(E)$ increases at higher E, reaching a plateau at $E \simeq 3.7$ eV. It is thus obvious that triplet generation occurs via two main processes. The first process is associated with thermalized singlet excitons and therefore has a step function E dependence at E_{op} similar to $\eta_{\text{PL}}(E)$. We identify this process as due to intersystem crossing, ISC, from the singlet to the triplet manifold occurring at times of order 1 ns [13,14], which mainly involves thermalized excitons. The other process, with an onset at $E \simeq 3.2$ eV is therefore due to hot excitons. We identify the second process as singlet exciton fission [15] ($Ex \rightarrow T\uparrow +T\downarrow$), which is operative at $E \gtrsim 2E_T$, where E_T is the triplet energy. We thus obtain from the higher $\eta_T(E)$ onset at 3.2 eV a value $E_T \simeq 1.6$ eV. The fit through the data points has been obtained [16] using singlet exciton fission with $E_T = 1.6$ eV, an energy dependent fission yield involving emission of the most strongly coupled vibrations using a Huang-Rhys ansatz and an inhomogeneous broadening for E_T.

A direct confirmation of the E_T value extracted above is the observation of a weak phosphorescence emission, Ph, from the lowest lying triplet state to the singlet ground state [17]. We have succeeded in measuring this emission band in quadrature (Fig. 1), where mainly long-lived emission components consistent with long-lived triplet excitons may be observed. The modulation frequency in Fig. 1 was $f \approx 3.5$ kHz to optimize the signal/noise ratio, and we plot $(PL)_Q/(PL)_{\text{in}}$ to correct for the system energy response; the uncorrected PL spectrum is also plotted for comparison. Figure 1 demonstrates that there exists a long-lived Ph emission band with a high energy onset at $E_T = 1.6$ eV, in agreement with E_T determination from the $\eta_T(E)$ spectrum in Fig. 2. It is also seen that the Ph emission spectrum extends to lower energies due to phonon replica.

We note that the singlet exciton energy $E_S \simeq E_{\text{op}} \simeq 2.6$ eV is much larger than E_T ($\simeq 1.6$ eV), with an energy difference $\Delta_{ST} = E_S - E_T \simeq 1$ eV. Since Δ_{ST} is determined by the exchange interaction, then this large Δ_{ST} value shows that $e\text{-}e$ interaction in mLPPP is relatively strong. Also since the $T - T^*$ transition is into the continuum band or lower, i.e., into the m^3A_g exciton [18], then we can get a lower limit estimate for the singlet exciton binding energy, $E_b(\text{min})$ in mLPPP from the relation $E_b(\text{min}) = E(T - T^*) - \Delta_{ST} = 0.3$ eV, which is in agreement with E_b ($\simeq 0.5$ eV) obtained from electroabsorption spectroscopy [11].

In Fig. 3 we show the polaron photogeneration quantum efficiency, $\eta_P(E)$, obtained by measuring $\Delta T_Q(E)/gI$ for the P_1 band at $\hbar\omega = 0.4$ eV (Fig. 1). We get the absolute value of η_P by normalizing the PMAS by σ of polarons extracted from doping induced absorption measurements [10]; we also found that $\eta_P(E)$ is temperature independent [9]. It is seen that $\eta_P(E)$ abruptly increases at $E =$
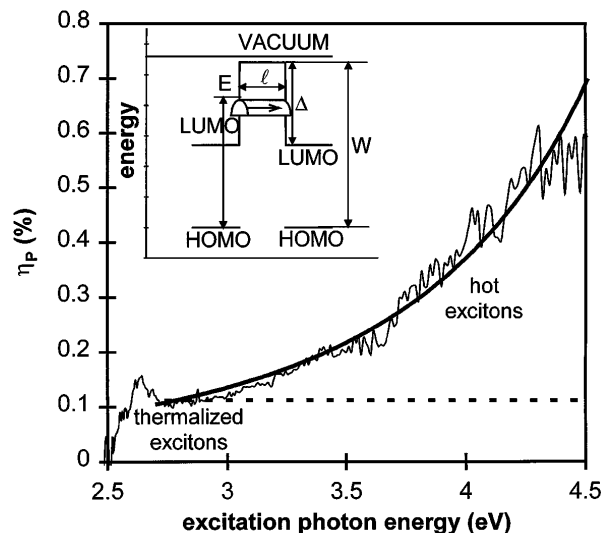

FIG. 3. The polaron action spectrum, $\eta_P(E)$. The two photogeneration processes due to hot and thermalized excitons, respectively, are assigned. The dotted line illustrates $\eta_P(E)$ separation into the two photogeneration processes. The bold line through the data points is a theoretical fit using an interchain tunneling model, as explained in the inset: HOMO (LUMO) are the highest occupied (lowest unoccupied) molecular orbital of two neighboring chains, $l(\Delta)$ is the interchain barrier potential width (height), and W is the energy difference between the HOMO and the vacuum level.

2.5 eV, similar to $\eta_{\text{PL}}(E)$ and $\eta_T(E)$. At $E > 2.85$ eV, however, $\eta_P(E)$ monotonously increases with E, where a saturation at high E similar to that found in $\eta_T(E)$ is not observed. We conjecture that $\eta_P(E)$ is composed from two contributions related to two different polaron photogeneration processes. One process is due to thermalized excitons and is thus independent of E, similar to $\eta_{\text{PL}}(E)$. We identify this process as thermalized exciton dissociation ($EX \rightarrow P^- + P^+$) at impurities and defects in the film, similar to the "extrinsic" process observed in cw photoconductivity, PC [19].

The second polaron photogeneration process is related to hot excitons and has thus a distinctive E dependence that increases at high E. For this, temperature independent, intrinsic process we suggest an interchain electron tunneling model (Fig. 3, inset). The electron and hole comprising a thermalized exciton are closely bound by a Coulomb binding energy of ≈ 0.5 eV. This makes their separation into free polarons very unlikely. At initially high E the electron, however, may tunnel to another chain (or chain segment) already during hot exciton thermalization, before the excess energy is completely released. The tunneling probability for the electron, $p(E)$, is given by

$$p(E) = \nu_0 \int_{E_{\text{op}}}^{E} e^{-(2l/\hbar)\sqrt{2m_e^*(\Delta+E_{\text{op}}-E')}}\, dE', \quad (2)$$

where l is the interchain tunneling distance, m_e^* is the electron effective mass, and Δ is the barrier height for tunneling, which is given by the energy difference between

the lowest unoccupied molecular orbital (LUMO) and vacuum levels: $\Delta = W - E_{op}$. In Eq. (2) ν_0 is the number of tunneling attempts per unit energy as the electron thermalizes from E to E_{op}. In this model $p(E_{op}) \simeq 0$ due to the large intrachain exciton binding energy. This is in agreement with the directly determined time evolution (with 100 fs resolution) of the exciton dissociation probability in mLPPP [20], which is 1 order of magnitude higher during hot exciton thermalization as compared to thermalized excitons. The following values for W, $l\sqrt{m_e^*}$, and ν_0 are extracted from the fit obtained to both $\eta_P(E)$ *spectrum* and *magnitude,* using Eq. (2), as shown in Fig. 3: We obtained $W = 5.5 \pm 0.5$ eV, which is in excellent agreement with electron affinity measurements in mLPPP [21], $l\sqrt{m_e^*} = 4 \pm 1$ Å $\sqrt{m_e}$ and $\nu_0 \approx 0.5$ eV^{-1}. The limits of m_e^* are $0.1m_e$ (conventional inorganic semiconductors) and m_e; for these values of m_e^* we obtained from $l\sqrt{m_e^*}$ determined above $l = 12$ Å and $l = 4$ Å, respectively. The experimentally determined neighboring interchain distance in mLPPP films is 20 Å [7] and may serve as an upper limit for l. From ν_0 and the maximum thermalization rate, $R_{th} = \Delta E / \Delta t$, taken to be $h\nu^2$ [22], where $h\nu \approx 180$ meV is the most strongly coupled vibration quantum (C=C stretching mode), we get a reasonable value for the attempt frequency to tunnel, $\nu_T = R_{th}\nu_0 \approx 0.1\nu$. We note that at high electric fields, F, of order 10^5 V/cm, however, polaron photogeneration in a single chain becomes possible and a similar exciton dissociation model may also explain the F dependence of $\eta(E)$ observed in PC measurements [23].

Interchain tunneling leads to the formation of coulombically bound polaron pairs on neighboring polymer chains. However, the PA bands P_1 and P_2 are due to free polarons as deduced from the observation of BR kinetics for these bands [9]. The dissociation of polaron pairs into free polarons occurs by hopping, which is only weakly temperature dependent. Based on a dielectric constant of 3.5 and an interchain distance of 20 Å, we calculate the interchain polaron pair binding energy to be ≈ 0.2 eV. This is of the same order of magnitude as the polymer energy inhomogeneity in mLPPP, and, therefore, the process of polaron pair dissociation into free polarons would not be activated. This is in agreement with the temperature independent $\eta_P(E)$ that we found here.

We thank U. Scherf and K. Muellen for the mLPPP powder and E. Ehrenfreund for useful discussions. The

[1] *Primary Photoexcitations in Conjugated Polymers; Molecular Excitons vs. Semiconductor Band Model,* edited by N. S. Sariciftci (World Scientific, Singapore, 1997).
[2] M. Liess *et al.,* Phys. Rev. B **56**, 15 712 (1997), and references therein.
[3] M. Ozaki *et al.,* Phys. Rev. Lett. **79**, 1762 (1997), and references therein.
[4] W. S. Fann *et al.,* Phys. Rev. Lett. **62**, 1492 (1989); B. Lawrence *et al.,* Phys. Rev. Lett. **73**, 597 (1994).
[5] U. Scherf and K. Muellen, Makromol. Chem. Rapid Commun. **12**, 498 (1991).
[6] S. Tasch *et al.,* Appl. Phys. Lett. **68**, 1090 (1996); A. Haugeneder *et al.,* Appl. Phys. B **66**, 389 (1998).
[7] G. Leising *et al.,* Proc. SPIE Int. Soc. Opt. Eng. **2852**, 189 (1996).
[8] W. Graupner *et al.,* Phys. Rev. B **54**, 7610 (1996).
[9] M. Wohlgenannt *et al.* (to be published).
[10] W. Graupner *et al.,* Solid State Commun. **91**, 7 (1994); Soc. Plast. Eng. Tech. Pap. **XLIII**, 1339 (1997).
[11] G. Meinhardt *et al.,* Synth. Met. **84**, 667 (1997).
[12] R. H. Friend *et al.,* Synth. Met. **84**, 463 (1997).
[13] S. Frolov *et al.,* Phys. Rev. Lett. **78**, 4285 (1997).
[14] J. W. Blatchford *et al.,* Phys. Rev. Lett. **76**, 1513 (1996).
[15] R. H. Austin *et al.,* J. Chem. Phys. **90**, 11 (1989), and references therein.
[16] M. Wohlgenannt *et al.,* in Proceedings of the International Conference on Synthetic Metals 98 [Synth. Met. (to be published)].
[17] H. F. Wittmann *et al.,* J. Chem. Phys. **101**, 2693 (1994).
[18] S. Mazumdar and M. Chandross, in Ref. [1], p. 384.
[19] M. Chandross *et al.,* Phys. Rev. B **50**, 14 702 (1994); S. Barth *et al.,* Chem. Phys. Lett. **288**, 147 (1998); A. Köhler *et al.,* Nature (London) **392**, 903 (1998).
[20] W. Graupner *et al.,* Phys. Rev. Lett. **81**, 3259 (1998).
[21] S. Tasch *et al.,* Phys. Rev. B **56**, 4479 (1997).
[22] Z. Vardeny and J. Tauc, in *Semiconductors Probed by Ultrafast Laser Spectroscopy,* edited by R. R. Alfano (Academic Press, New York, 1984), Vol. II, p. 23.
[23] V. I. Arkhipov, E. V. Emelianova, and H. Bässler, Phys. Rev. Lett. **82**, 1321 (1999).